Double Well Potentials and Quantum Phase Transitions in Ion Traps

A. Retzker, R. C. Thompson, D. M. Segal, and M. B. Plenio
Institute for Mathematical Sciences, Imperial College London, SW7 2PE, United Kingdom
and QOLS, The Blackett Laboratory, Imperial College London, Prince Consort Road, SW7 2BW, United Kingdom
(Received 16 June 2008; published 30 December 2008)

We demonstrate that the radial degree of freedom of strings of trapped ions in the quantum regime may be prepared and controlled accurately through the variation of the external trapping potential while at the same time its properties are measurable with high spatial and temporal resolution. This provides a new testbed giving access to static and dynamical properties of the physics of quantum-many-body systems and quantum phase transitions that are hard to simulate on classical computers. Furthermore, it allows for the creation of double well potentials with experimentally accessible tunneling rates, with applications in testing the foundations of quantum physics and precision sensing.

DOI: 10.1103/PhysRevLett.101.260504 PACS numbers: 03.67.−a, 37.10.Ty

Introduction.—Developing the ability to control and measure the dynamics of quantum-many-body systems with high accuracy as well as spatial and temporal resolution is a central goal in modern quantum physics. The recent development of ion trap technology, in particular, has enabled precise control of the internal and external degrees of freedom in strings of ions [1,2] which can be used for quantum information processing [3] as well as quantum simulations [4]. Theoretical schemes were proposed which use the phononic excitation to simulate scalar fields, either for the simulation of the spin boson model [5] or for the simulation of the vacuum [6]. In this context the longitudinal motion of the ions was considered. This leads to significant restrictions when using the motion to simulate quantum fields, both in the accessible dynamics (since quantum critical behavior cannot be reached directly) as well as in the measurement of local properties of the motion of the system, since only the global eigenmodes of the system may be accessed.

In contrast, here we demonstrate that the radial motion of the ions simulates a scalar field whose effective mass may be adjusted freely and precisely by the sole variation of the radially confining potential and that local and global properties of the radial motion can be measured accurately. In this approach the phonons of the crystal simulate the bosonic excitations of other fields. Crucially, this enables precise control near the symmetry breaking phase transition from a linear to a zigzag configuration (see Fig. 1). This transition is well known at the classical, high-temperature, level [7]. Advanced laser cooling techniques, however, make it possible to prepare the system close to its motional ground state and to control, manipulate, and probe it in the quantum regime, accessing its quantum phase transition and a large variety of linear and nonlinear scalar quantum fields. Furthermore, at zero temperature the ground state in the symmetry broken zigzag phase is degenerate and thus realizes an "intrinsic" double well (DW) potential whose parameters such as width and depth may be controlled precisely via the overall external confining potential without the need for micron-sized electrodes at high voltages. The latter approach may subject the ions to unwanted heating effects due to the proximity to the electrodes and would thus make the observation of quantum behavior challenging despite remarkable progress in segmented traps [8]. In the remainder of this Letter, we will demonstrate the versatility and promise of the proposed system by presenting several possible applications.

The Hamiltonian.—A system of N ions of mass m is subject to external harmonic potentials in the radial $(x - y)$ plane and axial (z) direction as well as their mutual electrostatic repulsion. The potential in the y direction is much stronger than in the x direction, reducing the problem to two spatial dimensions. This can be achieved both in linear ion traps and in Penning traps [9]. Then the Hamiltonian is

$$H = \sum_{i=1}^{N}\left[\frac{\hat{p}_i^2}{2m} + \frac{1}{2}m\omega_x^2\hat{x}_i^2 + \frac{1}{2}m\omega_z^2\hat{z}_i^2\right] + \frac{e^2}{4\pi\epsilon_0} \times \sum_{i>j}^{N}\frac{1}{\sqrt{(\hat{x}_i - \hat{x}_j)^2 + (\hat{z}_i - \hat{z}_j)^2}}, \quad (1)$$

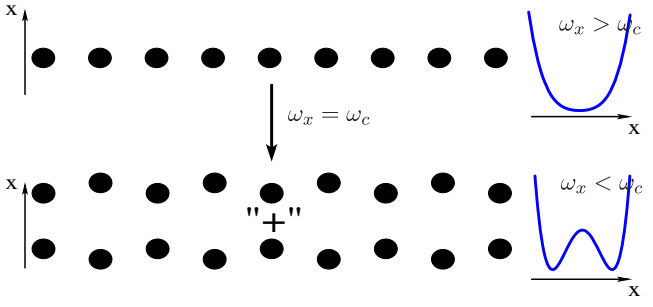

FIG. 1 (color online). Geometric transition between a linear and a 2D zigzag formation. The rotational symmetry has to be broken by the electrode structure. By controlling the external potential and hence the transversal oscillation frequency ω_x, a DW structure is realized after crossing the critical trapping frequency ω_c [see below Eq. (2)] for which the ground state is a superposition of the two zigzag configurations.

where $\hat{x}_i$ and $\hat{z}_i$ are components of the position operators of the ith ion. For the numerical examples in this work, we fix the strength of the confining potential such that the motional frequency in the axial direction is $\omega_z = 2\pi \times 1$ MHz. For each ω_x we may then determine the equilibrium arrangement of the electrostatic problem posed here. A fourth-order Taylor expansion of the potential yields the effective Hamiltonian

$$H = \frac{1}{2m}\sum_{i=1}^{N}\hat{p}_i^2 + \frac{1}{2}m\sum_{ij=1}^{N}\gamma_{ij}\hat{x}_i\hat{x}_j + \sum_{i=1}^{N}b_i\hat{x}_i^4 + \sum_{ij=1}^{N}(\alpha_{ij}\hat{x}_i^2\hat{x}_j^2 + \kappa_{ij}\hat{x}_i^3\hat{x}_j), \quad (2)$$

where the local terms are $\gamma_{ii} = \omega_x^2 - \sum_{i\neq j}\frac{e^2}{2m\pi\epsilon_0|z_i - z_j|^3}$ and $b_i = \frac{1}{4!}\sum_{i\neq j}\frac{9e^2}{4\pi\epsilon_0|z_i - z_j|^5}$ and for $i \neq j$ we have $\gamma_{ij} = \frac{e^2}{2m\pi\epsilon_0|z_i - z_j|^3}$, $\alpha_{ij} = \frac{9e^2}{16\pi\epsilon_0|z_i - z_j|^5}$, and $\kappa_{ij} = -\frac{3e^2}{8\pi\epsilon_0|z_i - z_j|^5}$; the coupling to axial modes which exists in third and fourth order has been omitted. While for $\omega_x \gg \omega_c$ the contribution of the nonlinear terms is small, by lowering ω_x we decrease γ_{ii} leading to an increase of $\langle\hat{x}^2\rangle$ and thus of the contribution of the nonlinear terms. Eventually, at a critical value $\omega_c \approx 3N\omega_z/(4\sqrt{\log N})$ (for $N \gg 1$) [11] of the external confining potential ω_x, a transition from a linear chain ($\omega_x \geq \omega_c$) to a zigzag configuration ($\omega_x \leq \omega_c$) takes place (Fig. 1). Now we present properties of the linear and zigzag phases and the phase transition between the two, demonstrating the versatility and controllability of the system.

Scalar quantum field with adjustable mass.—The Hamiltonian (2) describes a nonlinear scalar field on a lattice. The ions form a chain of coupled harmonic oscillators where each ion represents a lattice site whose motional excitations play the role of the excitations of the nonlinear field. The effective mass of the field, which is determined by the local potential, may be adjusted via the free parameter ω_x which, in turn, can be controlled by the choice of the external potentials. At the point of phase transition between the linear chain and zigzag formation (Fig. 1), the nonlinear terms in the Hamiltonian become important and the field becomes massless and thus critical. This allows for the exploration of critical phenomena in such systems. While entanglement properties of linear quantum fields, for example, have attracted considerable attention [12], nonlinear fields have proven largely inaccessible to analytical work so far. The setting we propose here allows for an experimental study of entanglement properties even in such nonlinear quantum fields which may differ from those of linear fields.

A linearized model for a chain of ions, i.e., the regime where $\omega_x \gg \omega_c$, is obtained by expanding $\hat{x}_i$ and $\hat{p}_i$ for the radial motion at site i into normal modes of frequency ω_n with annihilation and creation operators a_n and $a_n^\dagger$, respectively. Here $\hat{x}_i = \sum_n f_n^i(\hat{a}_n e^{-iw_n t} + \hat{a}_n^\dagger e^{iw_n t})\sqrt{\hbar/2mw_n}$ and $\hat{p}_i = -i\sum_n f_n^i\sqrt{\hbar m w_n/2}(\hat{a}_n e^{-iw_n t} - \hat{a}_n^\dagger e^{iw_n t})$, where f_n^i are the normal mode coefficients of the crystal. Then in the ground state $\langle x_i^2\rangle = \frac{1}{2}\sum_n (f_n^i)^2\hbar/mw_n$ and $\langle p_i^2\rangle = \frac{1}{2}\sum_n (f_n^i)^2\hbar m w_n$. At the phase transition between the linear and the zigzag configurations, one normal mode becomes massless; its frequency ω_n vanishes. In a linearized model the massless mode leads to diverging $\langle\hat{x}^2\rangle$, while $\langle\hat{p}^2\rangle$ remains finite. Hence, near the transition point the entropy of the harmonic oscillator at location i, which quantifies its entanglement with the remainder of the chain, diverges, satisfying $S_1^i(\omega_x) = \log(\sqrt{\langle x^2\rangle\langle p^2\rangle}/\hbar) \approx \log[|f_0^i|\sqrt{\langle p^2\rangle/(2\hbar m\omega_0)}]$. Since the lowest normal mode frequency $\omega_0^2 = \omega_x^2 - \omega_c^2$, we find $S_1(\omega_x) \approx -\frac{1}{4} \times \log(\omega_x^2/\omega_z^2 - \omega_c^2/\omega_z^2) = -\frac{1}{2}\log\omega_0/\omega_z$. Nonlinear effects, however, will prevent the entanglement entropy from diverging, thus presenting an interesting diversion from the behavior of linear fields.

Intrinsic double well potential.—In the symmetry broken phase (zigzag), the ground state is twofold degenerate so that the ion crystal realizes an intrinsic quantum mechanical DW potential. By controlling the external confining potential, we are able to set the values a and b of the effective potential seen by the ionic crystal of the form $V(x) = V(0) + \frac{1}{2}a(\omega)x^2 + \frac{1}{4}b(\omega)x^4 + \cdots$ resulting in an effective DW structure with a distance $d = 2(-a/b)^{1/2}$ between the two minima, while the width of the ground state of each well is $\Delta = [\hbar/(2\sqrt{-ma})]^{1/2}$. When $a^2/4b \approx \hbar\sqrt{-2a/m}$, each well is sufficiently deep to accommodate one energy level. Note that this potential is not a passive external potential but results from internal Coulomb forces together with the external potential. Importantly, measurable tunneling rates are achievable with experimentally realistic values for the external con-

TABLE I. The values at the optimal point of the transition for systems from three to seven ions, i.e., the point where the DW is created. The first three rows show the local frequency of each single well of the DW, the tunneling rate, and the distance between them at the optimal point. The distances are calculated for $\omega_z = 2\pi \times 1$ MHz and scale as $1/\omega^{2/3}$. The last row shows the value of the deviation of the frequency from the critical one at the optimal point, i.e., the frequency precision needed for the experiment. In order to reach this frequency precision, a voltage precision of 0.1 V in the ac as well as mV stability and precision on dc is needed (assuming an applied ac voltage of a few hundred volts and a dc potential of a few volts). These are achievable with current technology.

	3-ZZ	4-ZZ	5-ZZ	6-ZZ	7-ZZ
Local freq [2π kHz]	111	143	172	200	226
Tunneling rate [2π kHz]	26	34	41	48	55
Distance [nm]	594	341	339	282	270
Radial freq ($\omega_x - \omega_c$)[2π kHz]	2	2.4	3	3.4	3.6

fining potentials (see Table I). The crucial advantage of the present approach as outlined above is that it obviates the need for micron scale electrodes carrying high voltages. The mechanism proposed here opens a new route to the demonstration and control of DW quantum dynamics for ions and its application for the exploration of the classical-quantum boundary and as a system for interferometry.

Manipulation and measurement.—We now discuss methods to rotate the quantum state formed by the DW potential over the entire Bloch sphere, schemes to verify this manipulation, and ways of measuring coherence and tunneling rates in the DW potential.

The first approach maps the external dof of the ions into their electronic dof employing a laser on the red sideband defined by the transition frequency between the two lowest energy levels of the DW $|L + R\rangle$ and $|L - R\rangle$ (see Fig. 2) and thus realizing the following Hamiltonian: $H_{\text{int}} = \Omega_r(\sigma_- |L - R\rangle\langle L + R| + \text{H.c.})$, where σ_- is the lowering operator of the internal dof. The Rabi frequency Ω_r is proportional to $\Omega_r = e^{-\eta^2/2}\sin(kx)[1 + O(e^{-(xl/\Delta x)^2})]$, where η is the Lamb-Dicke parameter multiplied by the factor of the addressed ion in the normal mode, Δx is the width of the wave function of one well, and x_l is the distance between the two minima. Therefore manipulation of the external dof is achieved by a three step procedure: first mapping it onto the electronic dof, followed by its manipulation employing an on-resonance laser, and then subsequently mapping it back. Note that the system does not have to be in the Lamb-Dicke regime for this manipulation to work. The manipulation of the motional dof may also be achieved by Raman transitions $|\downarrow L\rangle \longleftrightarrow |\uparrow C\rangle \longleftrightarrow |\downarrow R\rangle$ (Fig. 2) leaving the internal spin state unaffected. Another way would be to apply an rf field on resonance with the energy between the $|L + R\rangle$ and $|L - R\rangle$ states.

An alternative approach uses our ability to move adiabatically back and forth across the phase transition. In this way we can generate any desired state in the DW potential by controlling the state in the single well potential. The ground state $|0\rangle$ ($|1\rangle$) of the single well evolves adiabatically into $|L\rangle + |R\rangle$ ($|L\rangle - |R\rangle$) in the DW. To remain adiabatic, the rate should be less than the minimal energy gap (which does not vanish as explained above) but higher than the decoherence rate. A numerical simulation at zero temperature (Fig. 3) shows that high fidelities can be achieved for transition rates that are smaller than the energy gap. It should be noted that it is only necessary to cool the zigzag (ZZ) mode since all others interact through nonlinearities whose effect can be seen to be small. Nonlinearities increase with the number of ions, and thus for large chains cooling should be necessary for all of the radial modes. The parameters were taken from Ref. [13], when we have scaled the damping rate by $(\omega_e/\Delta)^2$, where ω_e is the trapping frequency in Ref. [13] and Δ is the energy gap in our case (26 kHz). The procedure would be the following: preparing three ions in the motional ground state of the ZZ mode in the single well potential and adiabatically reducing the radial confinement until the system undergoes the phase transition into the ground state of the DW potential $|L + R\rangle$. For manipulation the potential can be adiabatically increased until the system is back in the single well and in the Lamb-Dicke regime, then applying a rf-π pulse to transfer the state into the internal dof, manipulating the system, mapping back, and finally transferring the system adiabatically to the DW state. Measuring can be done in an analogous way.

In order to investigate tunneling, the system could be prepared in the $|L\rangle$ state in the DW to be confirmed by position sensitive measurement. After $1/(26\text{ kHz}) \sim 30\ \mu$s the system should have evolved into state $|R\rangle$. By analyzing the statistics of an ensemble of measurements for one specific tunneling duration and increasing the duration stepwise by changing the external potential could allow one to see a sinusoidal oscillation of the probability

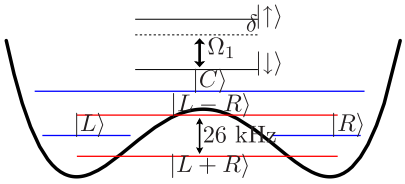

FIG. 2 (color online). DW energy levels for the three ions case. The DW potential shows the ground state ($|L + R\rangle$) and the first motional excited state ($|L - R\rangle$) of the ZZ mode. The inset shows the internal level structure. Since the energy gap is equal for both transitions, the manipulation can be done with one laser with Rabi frequency Ω_1 appropriately detuned to the red sideband with detuning δ. When the wave function of level $|C\rangle$ extends across both wells and whose energy is thus well above the gap between the two lowest lying states, this achieves a transition. The manipulation of the external (dof) may also be achieved by applying a rf drive, in which case the Rabi frequency is proportional to $3\omega_l/4x_l$.

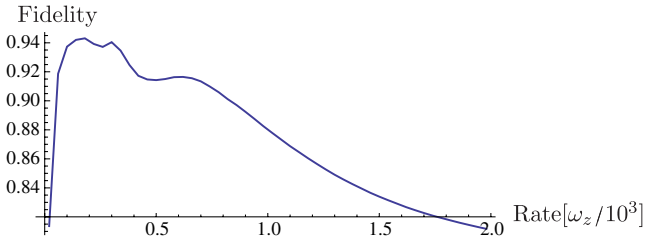

FIG. 3 (color online). Fidelity for the transition between the ground state of a single and DW potential for three ions (minimal energy gap is 26 kHz; see Table I). The initial state is the ground state of the single well potential. The wave function is evolved numerically, while the trapping potential reduces linearly in time. The figure shows the overlap with the ground state of the DW at the end of the sweep. The overlap decreases for high rates due to Landau Zener transitions and for low rates due to coupling with the environment.

to measure state $|L\rangle$ from which the coherence time could be deduced.

Realizations.—The ideas presented here may be realized in linear Paul traps as well as Penning traps. Linear Paul traps will exhibit micromotion when ions are displaced from the trap axis. Nevertheless, for small displacements, as discussed here, micromotion will lead to minor decoherence effects and a renormalization of the depth and width of the DW potential which is not significant. Penning traps, on the other hand, do not suffer from micromotion at all, and thus the crystal may be even less susceptible to decoherence. However, observations need to take place in a rotating frame in which the effect of the magnetic field is cancelled [14].

The realization of the DW potential described here could open the way to interferometry at the nanoscale. Ion traps have already been used as a measurement apparatus at the nanoscale [15] and DWs for single atoms, and Bose-Einstein condensates have been used for precise measurement in interferometry experiments [16,17]. For ions the DW structure is insensitive to linear and quadratic low frequency perturbations, since linear perturbations would shift the potential and quadratic ones will shift the transition point. An interferometry scheme which is realized by openings and closing the DW (like in [18]) potential could estimate the cubic parts of the trapping potentials. This interferometry experiment will measure the averaged cubic term, when the average is performed over the axial part of the potential. Thus by using the intrinsic DW potential created by the ion string, precise measurements of nonlinear electric and linear magnetic fields on the nanoscale would be possible while being insensitive to linear perturbations. Nonlinear terms of electric fields can be measured by observing dephasing of the spatial dofs, and linear terms of magnetic fields can be measured by using the magnetic levels. To measure the correlations of the gradients of the magnetic field, a magnetic sensitive state of the atomic part can be prepared. After opening and closing the trap, the collected phase difference during the procedure would manifest itself in crystal phonons. This phase difference $\langle \Delta\phi^2 \rangle$ is proportional to $\int dt_1 dt_2 \langle \nabla B(x_i, t_1) \nabla B(x_j, t_2) \rangle$. Thus the interferometric procedure would measure the $\langle \nabla B(x_i, t_1) \nabla B(x_j, t_2) \rangle$ or the $\langle \triangle E(x_i, t_1) \triangle E(x_j, t_2) \rangle$ correlations, where x_i and x_j are the locations of the ZZ ions. The scalability in this scheme is limited by the ground state cooling of the chain. On the one hand, single ion addressing is not needed in this scheme, and thus strong trapping frequencies are possible also for large number of ions; on the other hand, nonlinearities become larger with increasing strength, in which case a whole ion chain cooling is needed.

In conclusion, we have demonstrated that in the quantum regime the transversal motion of chains of trapped ions and its symmetry breaking configurational phase transition provide an ideal testbed for a variety of physical effects. These range from the properties of nonlinear lattice field models, the Kibble-Zurek mechanism, i.e., defect formation when traversing the phase transition, and, importantly, the possibility for the demonstration of coherent tunneling between degenerate ground states of the intrinsic DW potentials formed in the symmetry broken phase. The latter, when realized for trapped ions, opens the way to a series of interferometry experiments. The realization and verification of the above effects depend on the high level of control of the quantum dynamics and the very high measurement efficiency that is accessible in ion traps. Our work sets out a series of novel goals for ion trap research that are more accessible than full-scale quantum information processing.

We acknowledge support by the EU Integrated Projects QAP and SCALA, the EPSRC QIP-IRC, the EPSRC projects EP/E045049 and EP/P09572, and the Royal Society and helpful discussion with M. Hartmann and F. G. S. L Brandão.

[1] D. Leibfried *et al.*, Nature (London) **438**, 639 (2005).
[2] H. Häffner *et al.*, Nature (London) **438**, 643 (2005).
[3] J. I. Cirac and P. Zoller, Phys. Rev. Lett. **74**, 4091 (1995).
[4] D. Porras and J. I. Cirac, Phys. Rev. Lett. **92**, 207901 (2004); **93**, 263602 (2004); A. Friedenauer *et al.*, Nature Phys. **4**, 757 (2008).
[5] D. Porras *et al.*, Phys. Rev. A **78**, 010101(R) (2008).
[6] A. Retzker, J. I. Cirac, and B. Reznik, Phys. Rev. Lett. **94**, 050504 (2005).
[7] D. H. E. Dubin and T. M. ONeil, Rev. Mod. Phys. **71**, 87 (1999); D. J. Wineland *et al.*, Phys. Rev. Lett. **59**, 2935 (1987); G. Birkl, S. Kassner, and H. Walther, Nature (London) **357**, 310 (1992); S. Fishman *et al.*, Phys. Rev. B **77**, 064111 (2008).
[8] K. Abich *et al.*, J. Opt. B **6**, S18 (2004); S. Seidelin *et al.*, Phys. Rev. Lett. **96**, 253003 (2006); J. Labaziewicz *et al.*, Phys. Rev. Lett. **100**, 013001 (2008).
[9] Breaking the radial symmetry in a linear rf trap can be achieved by applying a dc potential to two opposing rods leading to a deeper potential along the direction between these rods (for the correct polarity). In the Penning trap this can be achieved by axialization [10].
[10] H. F. Powell, D. M. Segal, and R. C. Thompson, Phys. Rev. Lett. **89**, 093003 (2002).
[11] G. Morigi and S. Fishman, Phys. Rev. E **70**, 066141 (2004).
[12] K. Audenaert *et al.*, Phys. Rev. A **66**, 042327 (2002); A. Botero and B. Reznik, Phys. Rev. A **70**, 052329 (2004).
[13] D. M. Lucas *et al.*, arXiv:0710.4421.
[14] R. Thompson and D. Wilson, Z. Phys. D **42**, 271 (1997).
[15] G. R. Guthöhrlein *et al.*, Nature (London) **414**, 49 (2001).
[16] R. Fermani, S. Scheel, and P. L. Knight, Phys. Rev. A **73**, 032902 (2006).
[17] A. I. Sidorov *et al.*, Phys. Rev. A **74**, 023612 (2006).
[18] T. Schumm *et al.*, Nature Phys. **1**, 57 (2005).